Received: 8 January 2025 | Revised: 14 February 2025 | Accepted: 15 February 2025

DOI: 10.1002/pc.29689

RESEARCH ARTICLE

spe INSPIRING PLASTICS PROFESSIONALS Polymer COMPOSITES WILEY

Feasibility and performance evaluation of randomly oriented strand recycled composite skins in sandwich structures: A green cost-effective solution for aerospace secondary load-bearing applications

Yağız Özbek[1,2] | Abdulrahman Al-Nadhari[1,2] | Sinem Elmas[1,2] | Volkan Eskizeybek[3] | Mehmet Yıldız[1,2] | Hatice S. Sas[1,2,4]

[1]Sabanci University Integrated Manufacturing Technologies Research and Application Center & Composite Technologies Center of Excellence, Manufacturing Technologies, Sabanci University, Istanbul, Turkey

[2]Faculty of Engineering and Natural Sciences, Sabanci University, Istanbul, Turkey

[3]Department of Materials Science and Engineering, Faculty of Engineering, Çanakkale Onsekiz Mart University, Çanakkale, Turkey

[4]School of Mechanical, Aerospace and Civil Engineering, The University of Sheffield, Sheffield, UK

Correspondence
Hatice S. Sas, Sabanci University Integrated Manufacturing Technologies Research and Application Center & Composite Technologies Center of Excellence, Manufacturing Technologies, Sabanci University, Istanbul 34906, Turkey.
Email: h.s.sas@sheffield.ac.uk

Funding information
Türkiye Bilimsel ve Teknolojik Araştırma Kurumu, Grant/Award Number: 2244; Çanakkale Onsekiz Mart Üniversitesi, Grant/Award Number: FYL-2020-3375

Abstract

Despite the advantages of recycled randomly oriented strand (ROS) composites over recycled grinded ones, the warpage issue hinders their adaptation in the industry due to tolerance requirements. To address this challenge, ROS composites are incorporated into secondary bonded sandwich structures such that the core material ensures the straightness of the ROS composite skins. Additionally, atmospheric plasma activation (APA) is utilized to enhance the skin/core bonding to prevent skin separation under loading. The ROS composite skins are manufactured via vacuum-assisted hot press to achieve a cost-effective aerospace-grade quality. The structural integrity of the sandwich structure is assessed through flatwise tensile and edgewise compression tests, while the mechanical and thermomechanical performance is evaluated using flexural, impact, and dynamic mechanical analysis (DMA) tests. The flatwise tensile and edgewise compression tests confirm that APA effectively prevents core detachment, as evidenced by an average tensile strength of 2.28 MPa and an average compressive strength of 171.7 MPa. Moreover, the flexural and impact tests show that no premature skin failure occurs, supported by an average facing strength of 59.23 MPa in flexural testing and an average impact energy of 49.96 kJ/m^2. The DMA test indicates that most of the stiffness loss is due to the core material. This comprehensive analysis highlights recycled ROS composites as a sustainable and cost-effective alternative for quasi-isotropic skins in aerospace secondary load-bearing sandwich structures such as floors, doors, engine cowls, and spoilers.

Highlights

- The core material serves as a structural stabilizer, eliminating skin warpage.
- Flatwise tensile test proves the efficiency of APA treatment.
- Edgewise compression test shows warpage does not induce skin/core debonding.

• The absence of premature failure illustrates the robustness of the structure.

KEYWORDS

atmospheric plasma activation (APA), CF/PEKK, randomly oriented Strand (ROS), recycled, sandwich structures

1 | INTRODUCTION

Sandwich structures have increasingly replaced traditional materials across various structures, ranging from small components like control surfaces and leading edges to critical structural parts, such as nose caps and fuselages in heavyweight vehicles like spacecraft.[1] Typically, a sandwich structure consists of two thin but rigid face sheets and a lightweight core. Carbon fiber and glass fiber-reinforced polymer composites (CFRP and GFRP) in addition to Kevlar-reinforced laminates, are commonly used as face sheet materials because of their high specific stiffness and strength.[2] Carbon fibers possess the highest specific modulus and strength among all reinforcing fibers, making them ideal for high-performance applications.[3] Unlike glass and other organic polymer fibers, carbon fibers do not necessarily break under stress, offering greater durability and structural integrity.[4] Their exceptional fatigue resistance, thermal stability, and lower density further contribute to their widespread use in advanced composite structures. These inherent properties of carbon fibers make them ideal as face sheets in sandwich structures for aerospace applications.[5] For the core material, polyurethane foam and polymeric and aluminum honeycomb are often preferred due to their lightweight nature.[6] Among these, honeycomb cores typically offer superior strength and stiffness compared to foam cores.[7]

The honeycomb sandwich structure offers an optimal combination of high flexural rigidity, bending strength, thermal insulation, and energy absorption capacity while maintaining a low weight.[1,6,8,9] Additionally, various mechanical properties and performance characteristics can be tailored according to the end-use requirements by adjusting the material and architecture of the core as well as the thickness and type of the face sheets.[8] Honeycomb sandwich structures are frequently used in aircraft flight control surfaces, such as rudders, ailerons, spoilers, and also interior components like floors, doors, overhead storage bins, ceiling, and sidewall panels.[1,9] Nomex paper strip honeycomb cores are commonly selected in sandwich structures, especially favored in aerospace applications where weight reduction is critical, due to their exceptional lightweight properties and high mechanical performance.[10]

Sandwich structures can be assembled using either co-curing or secondary bonding processes.[11] The co-curing method involves a single curing process in which intermolecular diffusion of polymers takes place between the components.[12] Although co-curing offers the benefit of a single-step manufacturing process, it introduces complexity to process parameters to achieve skin consolidation, skin and core bonding, resin flow, and internal gas pressure within the core, all of which lead to reduced mechanical properties of the laminate.[13] The secondary bonding method involves two processes where the skins are first manufactured individually to achieve optimal structural properties and then bonded to the core material using an adhesive film, creating a cohesive structure.[7,12] The adhesive layer secures the skins to the honeycomb core, facilitating the seamless transfer of stress between the skins via the core, which is vital for balanced load distribution.[14] The bond between skin and honeycomb core is fundamental to the overall quality and structural integrity (especially flatwise tensile strength) of sandwich structures. A strong skin-core bond allows effective force transition across the entire structure; however, in honeycomb sandwich structures, the limited bonding area provided by the cell walls makes strong adhesion difficult to achieve. Thus, various surface treatment techniques can be employed to optimize surface conditions and enhance the surface energy and wettability of the skin material.[15] The skin/core adhesion becomes even more critical when recycled materials, mostly thermoplastic materials, are used due to their hydrophobic nature, which limits bond strength due to insufficient wettability. In order to overcome this issue, atmospheric plasma activation (APA) treatment is widely utilized in surface treatment processes, which has proved to enhance bonding performance in a highly effective, eco-friendly, and cost-efficient manner.[16] By exposing the thermoplastic skin surface to APA, hydrophilic groups are introduced, which increases surface energy and improves wettability. This transformation fosters stronger chemical bonds with the adhesive layer, thereby improving the adhesive bond strength between the skins and core of sandwich structures without causing any surface damage.[17]

With the growing adoption of sandwich structures in aerospace applications due to their numerous advantages, ensuring sustainable production has become a critical concern. Consequently, researchers have begun exploring the feasibility of incorporating recycled core materials into these structures to enhance environmental sustainability and reduce material waste. In the literature,

recycled core materials have been the focus of several studies where their mechanical behavior in the sandwich structures is investigated. Mandegarian et al. manufactured sustainable all-thermoplastic sandwich panels using glass/polypropylene composite skins and 100% recycled PET foam cores in their study.[18] Flatwise testing revealed a failure pattern characterized by both adhesion and substrate failure, indicating a strong bond between the skin and polyethylene terephthalate (PET) foam. Higher-density foam cores improved bonding with the polypropylene resin, leading to increased flatwise tensile strength. The high-density cores achieved a tensile strength of 0.85 MPa when using a 10 mm thickness of recycled PET foam core. Kassab and Sadeghian conducted a comparative study on the flexural properties of sandwich composites consisting of PET fibers/epoxy composite skins and different recycled PET cores.[19] By incorporating recycled PET honeycomb cores, their research presented an innovative approach to sustainable materials, emphasizing the potential of recycled plastics in structural applications. Their findings indicate that replacing PET foam cores with honeycomb cores leads to significant increases in bending stiffness (ranging from 137% to 151%) and ultimate load capacity (ranging from 62% to 151%). Moreover, they observed core shear failure under flexural loading, in contrast to high-density foam cores that primarily exhibited complex wrinkling failure modes. Hu et al. explored the manufacturing techniques and compression characteristics of three-dimensional sandwich structures with lattice cores, made using continuous carbon fiber reinforced thermoplastic polyether-ether-ketone (CCF/PEEK).[20] They introduced an innovative hot stamping technique specifically for fabricating CCF/PEEK lattice cores. They observed that the compressive strength and modulus of CCF/PEEK lattice structures are maximized with the $\pm 45^{\circ}$ stacking sequence of lattice cores and a strong quantitative match between experimental results and simulation predictions.

However, the feasibility of utilizing recycled skin materials in sandwich structures remains an area that is underexplored in the existing literature. In recent years, the recycling of thermoplastic composites has gained significant attention in modern engineering applications, as they offer greater recyclability compared to thermoset composites, which present substantial challenges in reprocessing and reuse.[21,22] Thermoplastic composites present several advantages, such as excellent resistance, high damage tolerance, reusability, and room temperature storage.[6,23,24] These properties make thermoplastic composites an attractive alternative to thermoset ones, providing both environmental and performance benefits. With growing concerns about environmental sustainability, the reprocessability of thermoplastic composites becomes increasingly important. Due to their ability to soften when heated and solidify upon cooling, thermoplastic composites can be repeatedly remelted and reshaped. This characteristic not only facilitates recycling and reduces waste but also allows for the recovery of high-value materials, making them an environmentally favorable option.[25,26] Composite scrap for recycling comes from two main sources: end-of-life post-consumer products, known as old scrap, and production waste generated during manufacturing, referred to as new scrap. These two streams provide a reliable supply of composite materials for ongoing recycling efforts.[26] Thermoplastic composite scraps can be recycled mechanically through shredding or grinding and reproduced again by aid of heat and pressure without additional treatment. Although this method is cost-effective, it often leads to reduced fiber lengths, which can compromise the mechanical properties of the recycled material. As a result, these recycled composites are typically proposed for secondary applications where no demanding performance is required.[27,28] These scraps can be utilized to manufacture randomly oriented strand (ROS) composite plates. ROS composite plates can be manufactured by different manufacturing techniques, compression molding under vacuum, and vacuum bag molding (VBO).[29] The vacuum-assisted compression molding process stands out as the best candidate for the out-of-autoclave (OoA) method, saving costs and time without compromising the performance of the manufactured composites. Moreover, the mechanical performance of ROS recycled composite plates does not deteriorate significantly as they fulfill the critical fiber length criterion, unlike recycled composite plates manufactured from the grinded composite waste. This places the ROS recycled composites as a green solution for aerospace secondary load-bearing applications.[30]

Poly-aryl-ether-ketone (PAEK) advanced thermoplastic polymer family is notable for its high performance and excellent properties, making it well-suited for aviation applications. Poly-ether-ketone-ketone (PEKK), a member of the PAEK family, is a popular candidate in aerospace structural applications because of its relatively low processing temperature compared to other advanced thermoplastic composites.[24,31] Several studies have researched the recycling of advanced thermoplastic composites. Selezneva and Lessard studied the tensile properties of CF/PEKK ROS composites with strand sizes from 6 to 50 mm, finding that ROS retains 75% of the modulus and 40% of the strength of quasi-isotropic specimens.[32] Leblanc et al. investigated the flexural properties of recycled CF/PEEK composites made from mixtures of virgin strands and consolidated scrap with different ratios.[33] Their study found that flexural strength decreased as the consolidated scrap content increased. In another study, the effect of strand length on the tensile properties of CF/PEEK ROS composites is examined.[34] The results showed that both tensile strength and modulus increased as strand length increased

from 10 to 150 mm. However, despite the advantages of ROS composite plates, the inhomogeneity of the strands distribution leads to an unbalanced composite layup causing warpage in the recycled structure.[32,35,36] This warpage poses serious geometrical obstacles hindering their adaptation in the aerospace industry. Nevertheless, to the best of the authors' knowledge, no previous studies have investigated the mechanical behavior of sandwich composite structures made with recycled ROS thermoplastic skins.

The aim of this study is to assess the applicability of ROS composites to serve as skins in sandwich structures for aerospace secondary load-bearing applications. To this end, the composite skins are manufactured by using shredded CF/PEKK slit tape waste via vacuum-assisted hot press. The vacuum-assisted hot press manufacturing process is selected to achieve aerospace-grade quality while maintaining cost efficiency. Having the skin composites manufactured, their surfaces are activated using APA treatment, promoting strong interface bonding and preventing skin/core separation due to the warpage of the ROS skins. The sandwich structure is then manufactured following the secondary bonding method using a thermoset adhesive film. Here, the core material also serves as a structural stabilizer, ensuring the straightness of the ROS composite skins. The skin/core adhesion strength is evaluated through flatwise tensile and edgewise compression tests to determine the likelihood of ROS composite skin separation. After verifying the bonding quality of the sandwich composite, its mechanical performance is investigated under flexural and impact loadings. Furthermore, the thermal stability of the sandwich structure is analyzed using DMA testing. This study introduces, for the first time in the literature, the application of thin ROS composite structures in the aerospace industry, effectively addressing the warpage issue and meeting tolerance requirements.

2 | MATERIALS AND METHODS

2.1 | Materials

For the manufacturing of recycled composite skins, unidirectional CF/PEKK slit tapes (Toray Cetex® TC1320) are utilized to produce randomly oriented strands, which are highly valued for their effectiveness in aerospace applications.[37] The slit tape material consists of PEKK resin reinforced with carbon fibers, with a processing temperature between 370 and 400°C and a width of 6 mm.[38] The unidirectional layup of these slit tapes demonstrates a tensile strength of 2410 MPa and a compressive strength of 1300 MPa. The resin content by weight is 34% (RC), and the consolidated ply thickness is approximately 0.14 mm (CPT). The material density is specified as 1.59 g/cm.[3] The recycled composite skins are manufactured via a vacuum-assisted hot pressing process in which Thermalimide E 002 vacuum bag (Airtech), Upilex-25S release film (Airtech), Loctite 770-NC release agent (UBE), Airflow800 breather cloth (Airtech), and A-800-3G vacuum band (Airtech) are used. In the manufacturing of sandwich composites, the core material, AHN-4120-1/8-3.0 aramid fiber/phenolic coated Nomex honeycomb, is sourced from KORDSA.[39] The thermoset adhesive film used to bond the recycled CF/PEKK composite skins to the Nomex honeycomb core is Scotch-Weld AF 163-2 K, produced by 3M Company.[40] Technical grade isopropyl alcohol (IPA), solid sodium hydroxide (NaOH) with a density of 2.13 g/cm^3 and 85 wt% phosphoric acid solution are supplied from Sigma-Aldrich for cleaning the aluminum blocks used in the flatwise tensile test equipment. Additionally, Scotch-Weld DP 490 epoxy structural adhesive from 3M Company is utilized to bond the flatwise tensile test specimens to the aluminum blocks.

2.2 | Methods

2.2.1 | Manufacturing of recycled ROS CF/PEKK composite skins

In our previous study, we investigated the effect of strand size on the mechanical properties of recycled CF/PEKK panels. The results reveal that strands cut with scissors to the dimensions of 45 × 6 mm^2 exhibit the highest tensile and compressive strength, and hence these strand dimensions are adopted in this study.[41] All the cut CF/PEKK strands are first washed and then dried in an oven at 80°C for 24 h. During this manufacturing stage, recycled CF/PEKK composite plates are manufactured using hot press techniques under vacuum bagging to achieve low void content. For this purpose, the strands are placed in a vacuum bag in a random arrangement, surrounded by breather cloth strips to facilitate air evacuation. Additionally, the breather cloth strips are set to ensure that the manufactured plates measure 320 × 320 mm^2 in length and width, respectively. Approximately 162.5 g of the prepared CF/PEKK strands are used to obtain composite plates with an approximate thickness of 1 mm. Furthermore, to provide smooth separation of the manufactured plates, two release films—each coated with four layers of release agent—are placed between the CF/PEKK strands and the vacuum bag. The vacuum bag is then sealed and vacuumed for 30 min before consolidation. Initially, the vacuum-bagged CF/PEKK strands are heated to 170°C at a pressure of 0.25 bar. The temperature is increased to the processing temperature of 380°C while simultaneously raising the pressure to 20 bars. The dwell time is then

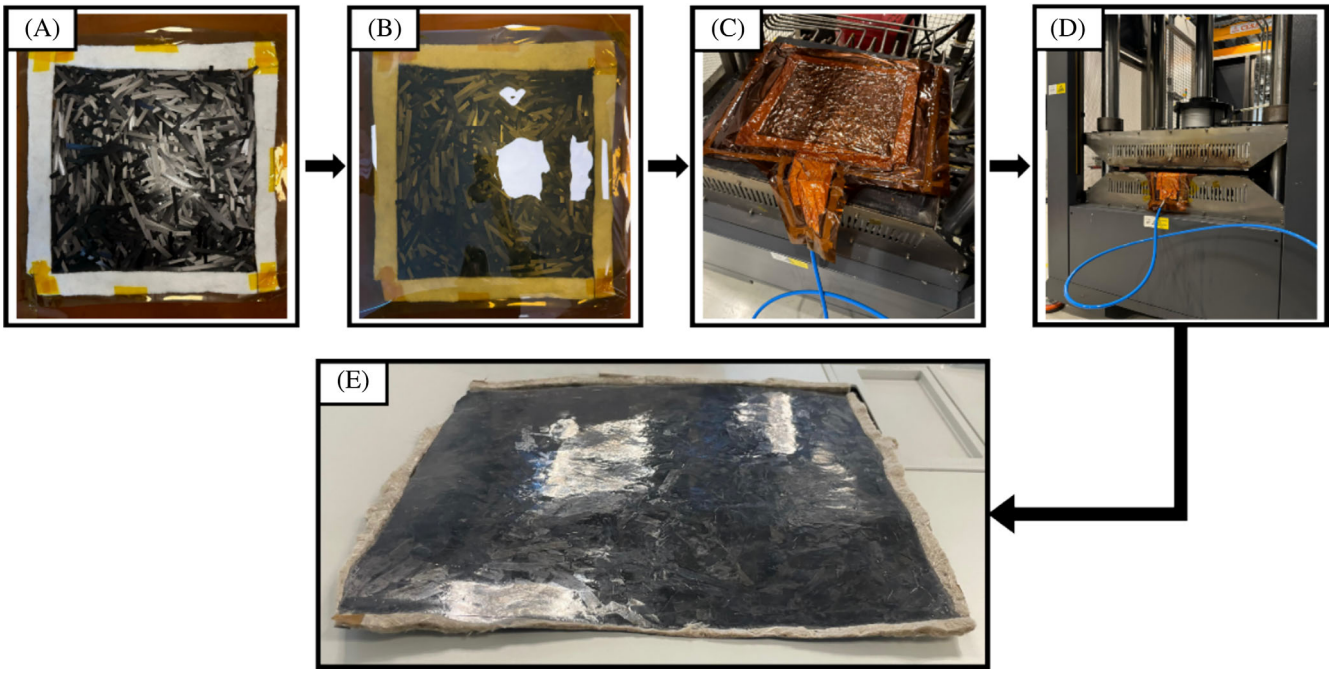

FIGURE 1 (A) Preparation of the recycled composite frame, (B) application of release films, (C) waste carbon fiber (CF)/poly-ether-ketone-ketone (PEKK) strands under vacuum bagging, (D) hot press process for consolidation of thermoplastic strands, and (E) the warpage of the recycled randomly oriented strand (ROS) CF/PEKK composite plate.

maintained at approximately 30 min under these conditions. The final step involves a gradual cooling phase, maintained below the glass transition temperature of approximately 160°C, to complete the manufacturing process of recycled ROS CF/PEKK composite skins. Figure 1 shows the manufacturing steps (Figure 1A–D) and the warpage of the produced ROS CF/PEKK plate (Figure 1E), while Figure S1 illustrates the hot press parameters, including temperature, pressure, and time. To obtain the specified final dimensions of 310 × 310 mm,^{2} recycled composite plates are trimmed using the KUKA KR-16–2 CF robotic water jet, followed by a drying process at 75°C overnight.

2.2.2 | Sandwich composite manufacturing

The manufacturing flowchart of the sandwich composites is shown in Figure 2. Once the recycled CF/PEKK composite skins are manufactured, the Nomex honeycomb, with a thickness of 9.84 mm (Figure 2A) is precisely cut using the ZÜND G3-L3200 digital cutting machine. The core material undergoes a drying process overnight at 75°C to remove moisture. In the preparation of the adhesive film, Scotch-Weld AF 163-2 K adhesive films (Figure 2B), initially stored at −18°C, are kept at a controlled temperature of 4°C overnight to prevent moisture accumulation. The adhesive film is then conditioned at room temperature for 30 min prior to cutting. The film is cut to the required dimensions using the same cutting machine employed for the Nomex core. Next, to enhance adhesive performance at the interface between the recycled skins and core parts, optimal APA process parameters for the recycled CF/PEKK composite plates are applied (Figure 2C). After cleaning the surfaces of the recycled skins with IPA, the parameters referenced in the literature include a nozzle distance of 15 mm, a scan speed of 40 mm/s, and three scans applied to both the top and bottom recycled composite skins. Following this set of parameters, the total surface free energy (SFE) of the composite skin increases from 40.73 to 70.26 mJ/m.^{2} This enhancement is primarily due to a significant increase in the polar component of SFE, while the dispersive component remains largely unaffected.[16] Following the application of the APA to the skin surfaces, Scotch-Weld AF 163-2 K adhesive films are implemented on the activated surfaces. Then, the Nomex honeycomb core is set between the skins, which have adhesive films, and the skin/core assembly is placed in an LP-MH4H50/MSE manual hot press machine for the adhesive curing process. The temperature is gradually raised from 20°C to 125°C at a rate of 5°C per minute, while the pressure remains constant at 2 bar. Once the curing temperature of 125°C is reached, the pressure is increased to 2.75 bar, and the adhesive is allowed to cure for a dwell time of 60 min. Upon completion of the curing process, the sandwich composite forms a unified structure (Figure 2D).

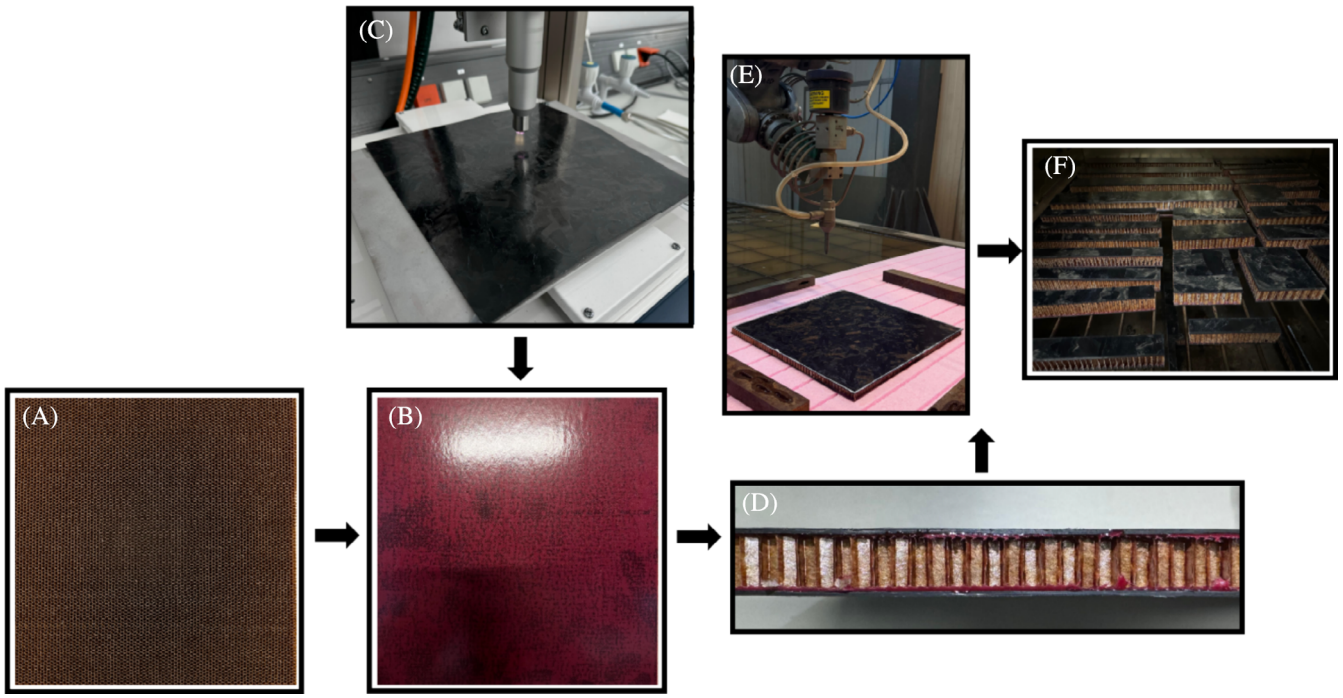

FIGURE 2 The manufacturing steps of sandwich composite structure. (A) Nomex core, (B) Scotch-Weld AF 163-2 K adhesive film, (C) application of APA treatment on recycled CF/PEKK skin, (D) sandwich composite structure, (E) water jet cutting, and (F) drying process in the oven.

To ensure compliance with all dimensional test requirements, the sandwich composite structure is precisely cut using a water jet, maintaining dimensions within the specified tolerance limits outlined in the relevant test standards (Figure 2E). Following cutting, the test specimens are dried overnight at 75°C to remove any moisture absorbed during the process (Figure 2F).

2.3 | Characterization and mechanical tests

The flatwise test equipment consists of two aluminum blocks, between which the test specimens are subjected to tension. Therefore, ensuring proper adhesion of the specimens to the aluminum blocks is a crucial parameter. Proper surface preparation of the aluminum blocks and precise adhesive application are significant for flatwise tensile testing. These steps ensure test validity by inhibiting failures in the epoxy between the aluminum blocks and the test specimen.[42] The aluminum alloy blocks are subjected to a cleaning process following ASTM D3933 standards to improve the bonding of the specimens to the testing fixture. This procedure involves multiple cleaning stages, including alkali and acid cleaning.[43]

The flatwise tensile test is performed on sandwich composite structures to assess the bonding performance at the core-skin interface. Following the ASTM C297 standard for flatwise tensile testing, three specimens of sandwich composite structures were precisely cut using a water jet to dimensions of 50 × 50 mm^2 and a thickness of 11.50 mm. The configuration for the flatwise tensile test of the sandwich composite structure is depicted in Figure 3. After the defined APA parameters are implemented on the surface of the sandwich specimens, 3M Scotch-Weld DP 490 epoxy structural adhesive is applied to both the aluminum blocks and the sandwich composite specimens. The specimens bonded to the aluminum blocks are then allowed to cure for 24 h at room temperature.

The flatwise tensile testing of composite sandwich specimens is performed using an INSTRON model 5982 testing machine, which has a maximum load capacity of 100 kN and operates at a speed of 4.00 mm/min at room temperature.

Following ASTM C364 guidelines, five edgewise compression sandwich composite test specimens are prepared to the specified dimensions of 80 × 25 $mm.^2$ The INSTRON 5982 testing machine is employed for this purpose, with the gauge length set at 10 mm. The crosshead displacement rate is consistently maintained at 0.50 mm/min at room temperature. The demonstration of the edgewise compression test setup is presented in Figure 4.

In accordance with ASTM C393, four sandwich composite specimens for a 4-point (4 pt) bending test are prepared with dimensions of 230 × 30 mm^2 for length and width, a core thickness of 9.84 mm, and a total sandwich

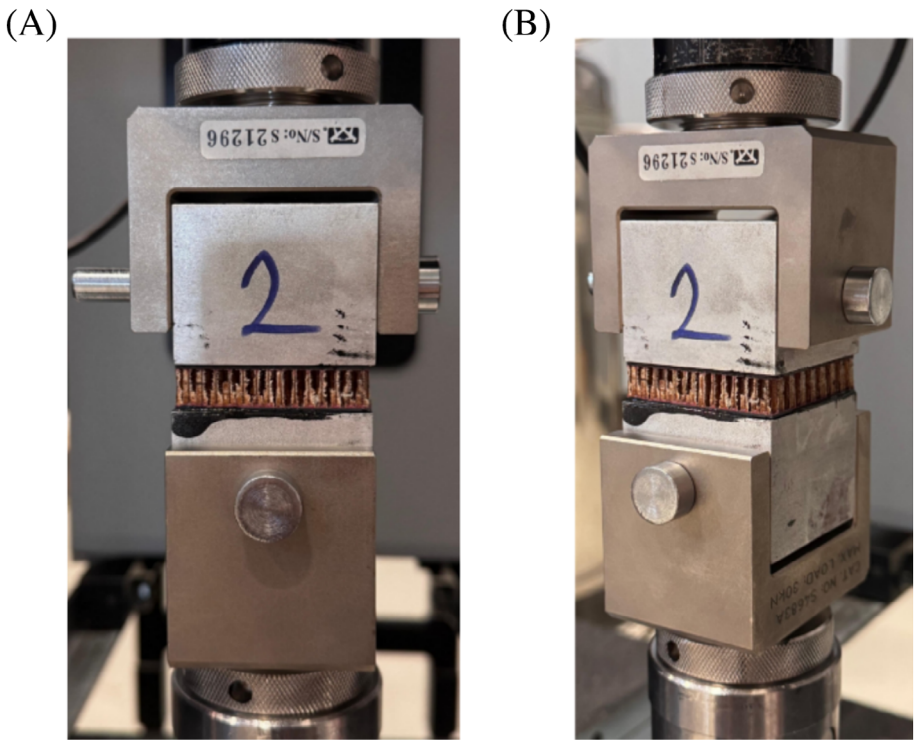

FIGURE 3 The illustration of flatwise tensile testing: (A) front and (B) isometric views.

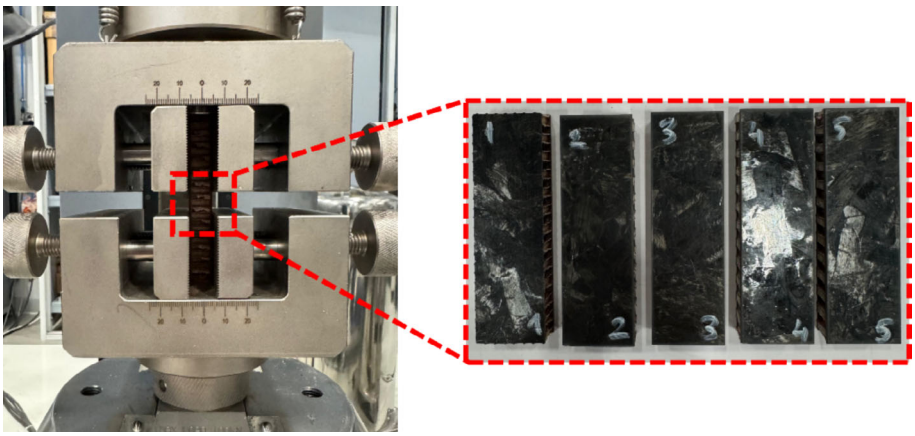

FIGURE 4 The installation of the sandwich composite structure in the edgewise compression test equipment.

structure thickness of 11.50 mm. The bending test for these specimens is conducted using an INSTRON model 5982 testing machine, with a span distance of 180 mm, a distance of 90 mm between the two applied loads, and a testing speed of 6.00 mm/min at room temperature. The arrangement for the 4-point bending test of the sandwich composite structure is shown in Figure 5.

The Charpy impact test is carried out to evaluate the impact resistance and durability of sandwich composite structures. According to the ISO 179 standard, five impact test specimens are prepared using waterjet cutting, each measuring 127 mm in length, 12.70 mm in width, and 11.50 mm in thickness. During testing, the hammer of the impact test apparatus is positioned to strike the recycled skin section of the unnotched specimens, as shown in Figure 6.

CFRP/Nomex sandwich composites are utilized in aircraft cowls, where they are exposed to elevated temperatures during engine operation.[44] Therefore, understanding the thermomechanical behavior of ROS/Nomex is essential. To evaluate this, dynamic mechanical analysis (DMA) is employed to assess the thermal and mechanical performance of the sandwich composite structures under varying temperature conditions. This technique allows for the measurement of mechanical properties in relation to time, temperature, and frequency.[45] Three specimens are prepared with dimensions of $55 \times 10\ mm^2$ for length and width, respectively. The tests are conducted using a Mettler Toledo DMA/SDTA861e instrument, following the dual cantilever mode. The experimental procedure involves a temperature range from 25 to 200°C, with a heating rate of 3°C per minute and a frequency of 1 Hz.

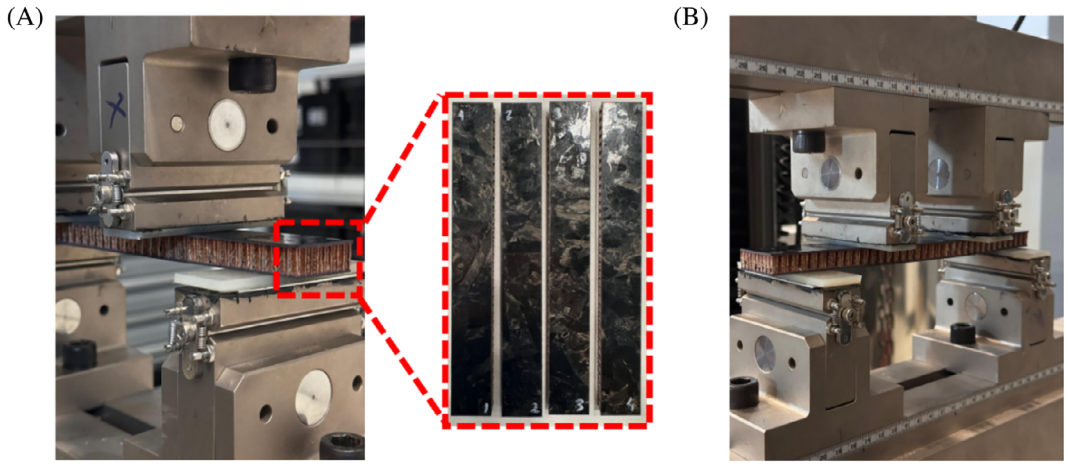

FIGURE 5 (A) 4-point bending test specimens of sandwich composites and (B) perspective view of the bending test setup.

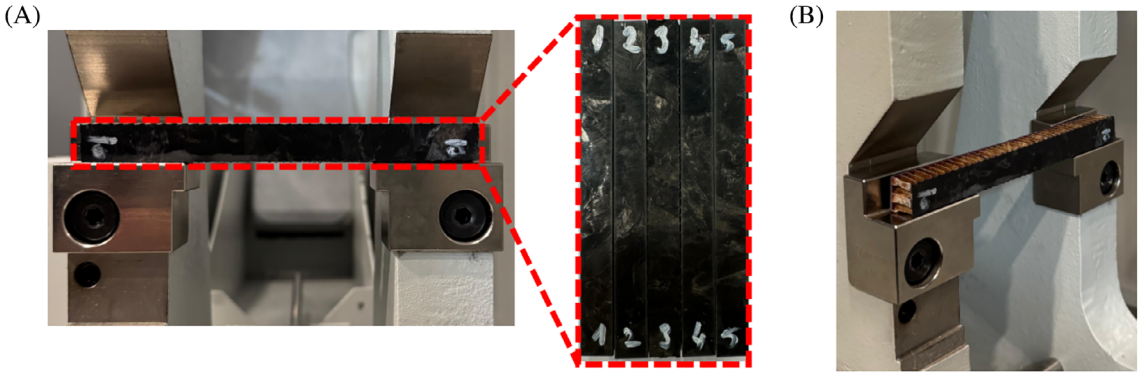

FIGURE 6 (A) Frontal view and (B) perspective view of the impact test configuration.

The load transfer capability of sandwich composites is significantly influenced by the quality of the bonding interface between the core and skin components. Therefore, following the manufacturing process, the distribution of the adhesive is analyzed using a Nikon SMZ800N Stereo Microscope at various magnifications. In addition, after the impact test, a microscopic analysis of the fractured specimens is conducted to examine the failure of the skin and core components. This is performed using a Leo Supra 35VP field emission scanning electron microscope (FE-SEM) at an accelerating voltage of 3 kV, under varying magnifications. To enhance electrical conductivity, a thin layer of Pd/Au is deposited onto the SEM specimens.

3 | RESULTS AND DISCUSSION

3.1 | Microscopic analysis of adhesive morphology

Microscopic images of the CF/PEKK Nomex sandwich composite specimen demonstrate a uniform and homogeneous distribution of adhesives along the skin/core cross-sectional interface (Figure 7). Robust bonding capability between the recycled skins and the core is achieved through the APA process, which enhances the wetting properties of the recycled skins prior to the sandwich manufacturing process. Enhancements in adhesive bonding led to better mechanical performance of the overall sandwich composite structure, as will be discussed in the test results.

3.2 | Flatwise tensile test results

Flatwise tensile testing evaluates the bonding performance between the skin and core, as well as the core strength of sandwich structures.[46] Figure 8A shows the results of the flatwise tensile test, displaying the curves of tensile stress versus displacement. The results show that the specimens exhibit linear behavior up to the ultimate tensile strength, where crack initiation takes place in the Nomex honeycomb. All specimens exhibit their ultimate tensile strength values at a tensile displacement of approximately 0.6 mm. This stable tensile displacement

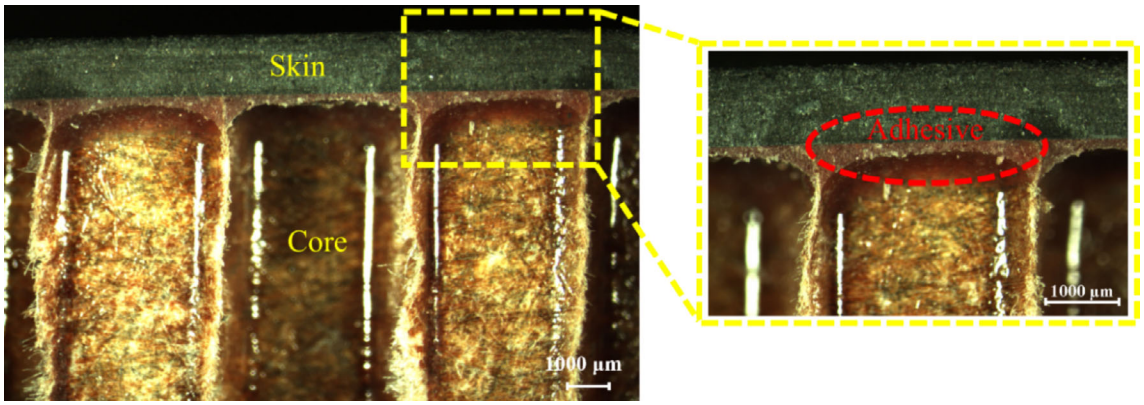

FIGURE 7 Demonstration of homogeneous adhesive distribution at the skin/core interface.

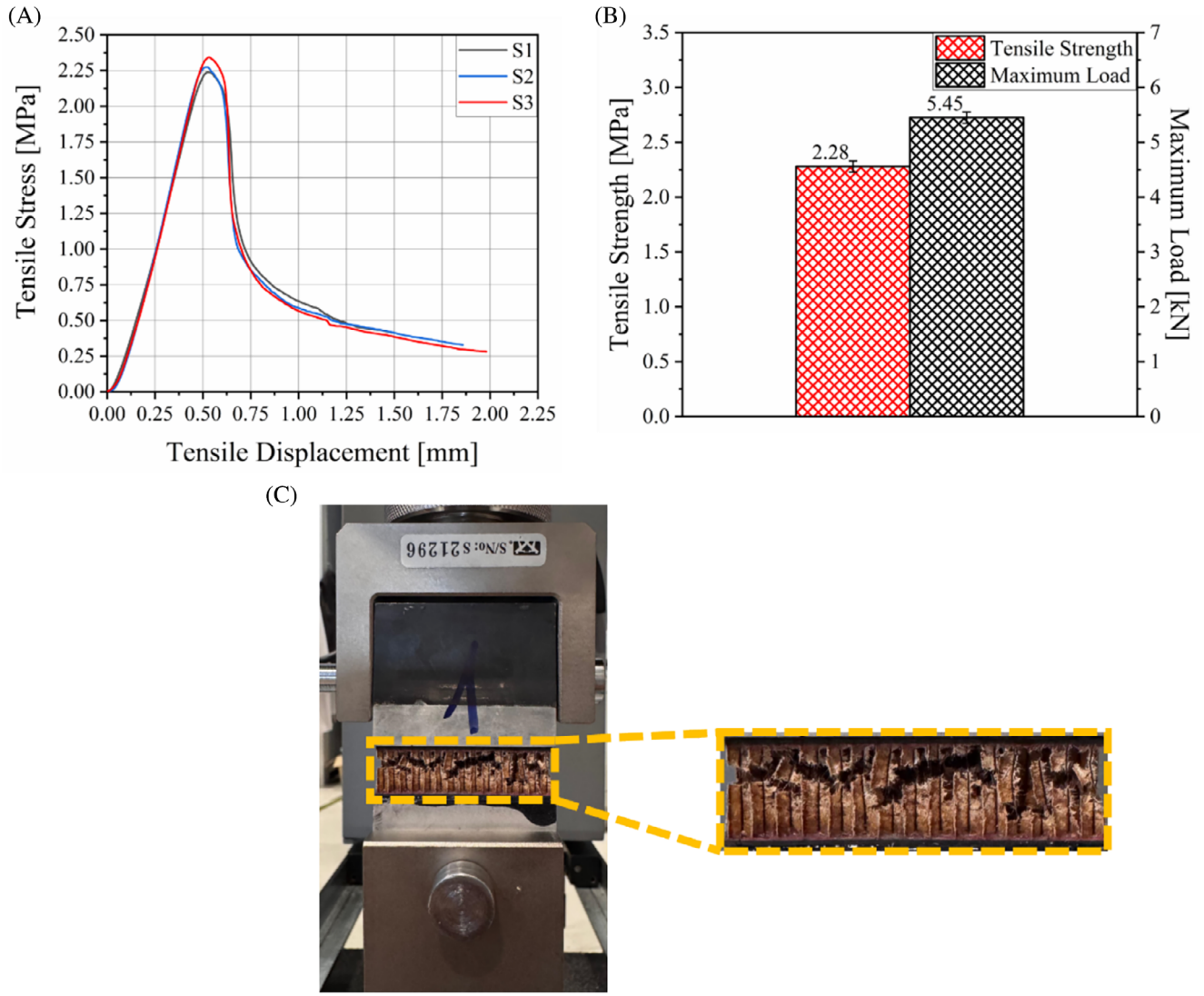

FIGURE 8 (A) Tensile stress-displacement curves, (B) average tensile strength and maximum load values of sandwich composite specimens, and (C) the crack propagation path of the honeycomb core after flatwise tensile test.

promotes consistency in the results. However, complete failure and separation do not occur instantaneously; instead, cracks gradually propagate through the honeycomb, causing a substantial loss in the load-carrying capacity of the core material, exhibited by the tensile stress drop.[47] The severity of the stress drop lessens as crack propagation becomes

more energy-intensive due to the expanding damage area. The sandwich composite structures demonstrate an average tensile strength of 2.28 MPa and an average maximum load capacity of 5.45 kN, as illustrated in Figure 8B. Liu et al. conducted flatwise tensile tests on sandwich composites made of carbon fiber/epoxy skins and a Nomex honeycomb core, reporting an average tensile strength of approximately 2.13 MPa.[48] In addition, our previous study reported an average tensile strength of 2.40 MPa from flatwise tensile tests on sandwich composites, where APA treatment was applied to the CFRP skin prior to its assembly with the Nomex core.[15] These results reveal comparable flatwise tensile values of the sandwich composite to those reported in the literature, despite the lower bonding performance of PEKK. This improvement can be attributed to APA activation, which significantly enhances the surface free energy of PEKK, resulting in better bonding performance. Specifically, the etching effect of APA treatment creates micro-grooves on the treated surface, enhancing mechanical interlocking. Additionally, APA treatment increases the oxygen atomic concentration on the surface, promoting the formation of chemical bonds.[49] This is also apparent in the failure behavior of recycled composite specimens, where failure occurs within the core without separating from the interface between the core and skins, as illustrated in Figure 8C. Moreover, the crack propagation within the honeycomb renders a curvilinear path rather than a linear one, implying mixed-mode crack propagation, which requires higher energy. This indicates that the load transfer capability between the skin and the core materials is improved.

3.3 | Edgewise compression test results

Figure 9 presents the edgewise compression test results along with the failure modes of the sandwich specimens. The compressive stress–strain curves, provided in Figure 9A, show that all the specimens behave similarly under compression. It can also be seen that the variation in compressive strength is lower than the variation in compressive strain. The average values of compressive strength and strain are depicted in Figure 9B. The average compressive strength and strain are calculated as 171.7 MPa and 1.26% with coefficients of variation of 7.8 and 12.75, respectively.

In the edgewise compression test, the composite skins serve as the primary load-carrying components, whereas the core material provides structural stability that helps in buckling resistance. This setup, as well as the introduction of recycled thermoplastic CF/PEKK composite skins, introduces complexity in the failure modes. That is, the variation in fiber angle within recycled CF/PEKK composites causes strain distribution nonuniformity across the specimen, leading to location-specific failure modes. Therefore, to better understand the failure mechanisms, the post-fracture images of the specimens should be investigated. Figure 9C shows that damage takes place within a contained region and does not extend throughout the specimen. Generally, it can be seen that the skin/core bonding is maintained in all the specimens, regardless of the specimen's failure mode. This proves that APA is successful in enhancing the structural integrity of the sandwich structure by creating new and/or increased hydrophilic functional groups during the bombardment of the surface of interest with the energized gas ions and free radicals in the plasma. This improves interfacial chemical bonding, which prevents skin detachment due to warpage.

Regarding the failure modes, specimens 1, 3, and 5 failed due to the buckling of one of the skins, which is accompanied by a compressive failure of the core material. The reason behind the buckling of a single side is the local anisotropy of the recycled skin. Specifically, damage is initiated at the position where the fiber orientation is the least favorable. On the other hand, specimens 2 and 4 failed due to the failure of both skins under compressive stress, while the core material remained intact, which increases the compressive strain. The intactness of the core material and the strong skin/core bonding prevent catastrophic failure in specimens 2 and 4 allowing them to continue carrying loads beyond their maximum compressive strength values, as seen in Figure 9A.

3.4 | Flexural test results

By analyzing the mechanical behaviors of the fiber composite skin and core components, theoretical estimates can be derived for the failure load, stress–strain relationship, and load-deflection behavior of sandwich composite structures subjected to flexural loads.[50] Common failure mechanisms observed in these structures under bending loads include skin compressive or tensile failure, as well as core shear failure.[51,52] In the mechanical evaluation of sandwich composite structures, it is typically assumed that the core primarily supports shear loads, while the skins are responsible for bearing tensile and compressive loads during flexural loading.[53]

Figure 10 presents the test results and the fractographic images of the 4–pt bending test. By analyzing the load-strain curve of all specimens, it can be concluded that each specimen undergoes four loading stages, as demonstrated in Figure 10A. In stage 1, the load increases linearly with respect to displacement, which means that no damage takes place in this stage. Stage 2 marks the onset

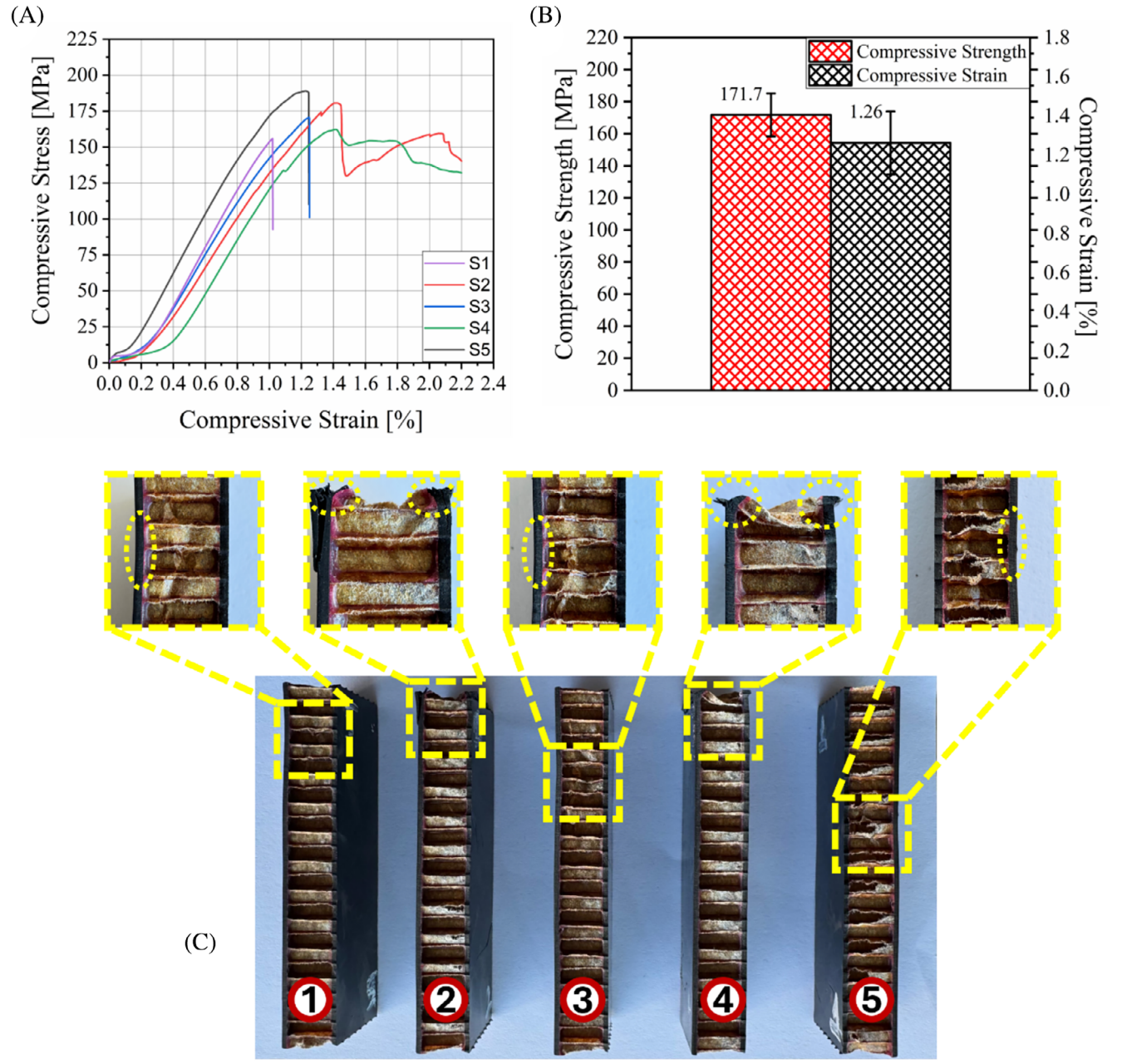

FIGURE 9 (A). Compressive stress–strain curves, (B) average compressive strength and compressive strain values of sandwich composite specimens, and (C) failure modes of the specimens.

of damage accumulation in the core material, resulting in a reduction in stiffness, although it remains constant throughout this stage. The constant stiffness in stage 2 hints that the damage accumulates in a steady and controlled manner. Stage 3 begins with the failure of the core material, causing a drop in load values. Finally, in Stage 4, the load starts to increase again gradually, resulting in high deformation as the structural support of the core material is absent and the upper and lower composite skins take on the load. Stage 4 ends with the ultimate failure of the specimen, resulting in a sharp decline in load values. The fractographic images in Figure 10C show the failure modes of the core and the skin materials. It can be seen that the core fails in shear mode, featuring multiple shear bands highlighted by the yellow arrows. This observation supports the earlier discussion on controlled damage accumulation. On the other hand, the skin fails under compressive stress without skin/core debonding, which results in a sharp drop in load value at the ultimate failure of the specimen. In Figure 10B, a bar depicts the average facing strength of 59.23 MPa with a coefficient variation of 5.58, as well as a core shear yield strength of 1.26 MPa with a coefficient variation of 6.9. These values are calculated using Equations (1) and (2).[54]

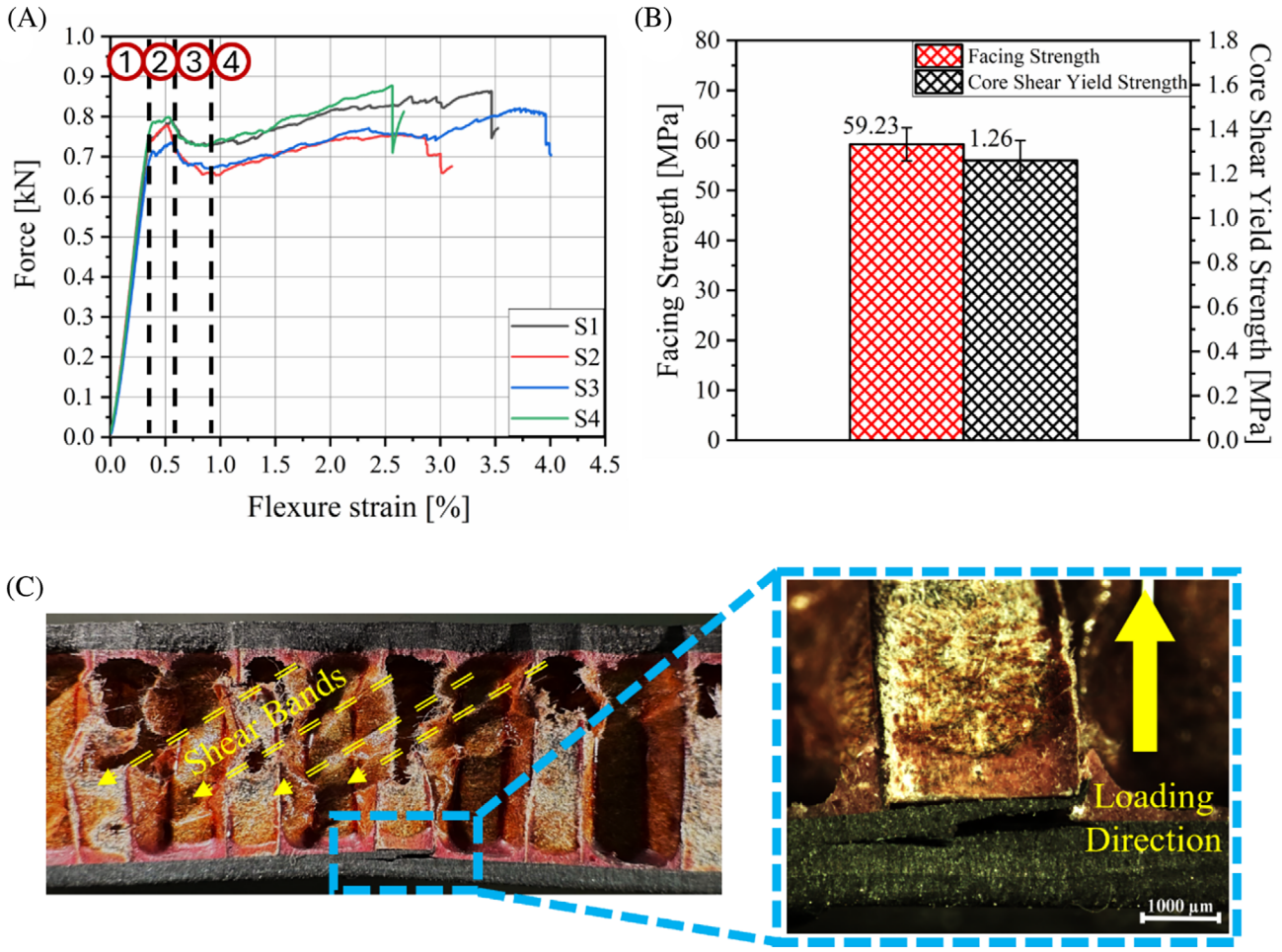

FIGURE 10 (A) Force-flexure strain curves and (B) average facing strength and core shear yield strength values of sandwich composite specimens, and (C) post-fracture images of the 4-pt bending test specimen.

$$(\sigma)_{4p} = \frac{1}{8}\frac{S(Pi)_{4p}}{bh_s(h_c + h_s)}, \quad (1)$$

$$(\tau_c)_{\max} = \frac{(P_y)_{4p}}{2b(h_c + h_s)}, \quad (2)$$

where $(Pi)_{4p}$ and $(P_y)_{4p}$ denote the load value at the first sharp drop of the load–displacement slope and 2% offset yield strength, respectively. S represents the sample support span distance. The parameters h_s and h_c correspond to the thickness of the face sheet and core material, respectively.

Naresh et al. conducted a 4-pt bending test on sandwich structures composed of CFRP face sheets (1 mm thick, made of epoxy resin reinforced with woven carbon fiber) and a Nomex core (10 mm thick). Their results indicate a face sheet bending stress of 35.48 MPa and a core shear stress of 0.93 MPa.[54] The utilization of recycled ROS CF/PEKK skins in sandwich structures demonstrates better flexural properties than thermoset counterparts of the same thickness. In addition, Zhu et al. performed flexural tests on Nomex core sandwich composites and reported an average shear strength of 0.91 MPa, which also supports the flexural results of this study.[55] This can be attributed to the fact that the primary load-bearing capacity originates from the type of skin material and its properties, which significantly influence the overall performance of the sandwich structure.

3.5 | Charpy impact test results

The Charpy test is essential for evaluating the toughness of materials under impact loading, as it quantifies the energy absorbed by a material before failure. This parameter is particularly important for assessing the mechanical performance of sandwich composites.[56] During flatwise Charpy impact testing, the load is applied along the thickness direction of the sandwich structure. The fracture starts at the impact point and then propagates through both the core and the bottom skin.[57] The average

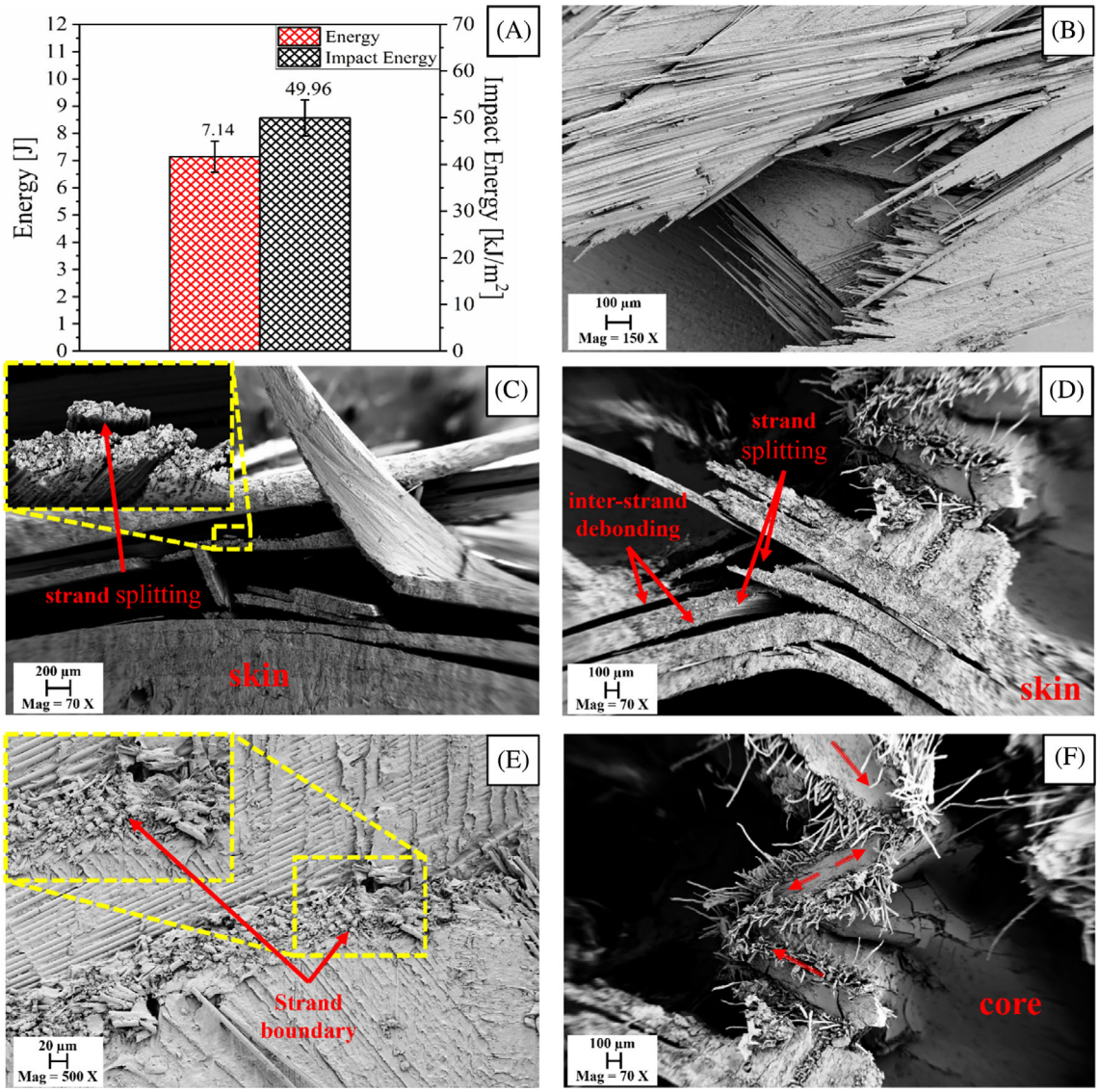

FIGURE 11 (A) Average energy (J) and impact energy (kJ/m^2) values, (B) scanning electron microscopy (SEM) image showing the strand orientation of the sandwich composites, and (C–F) SEM fractographic images of damaged sandwich impact specimens.

energy and the average impact energy values of five tested sandwich composite specimens are 7.14 J and 49.96 kJ/m,^{2} respectively, as shown in Figure 11A. The measured average impact energy value closely aligns with a study in the literature that reported a value of 54.4 kJ/m^2 for sandwich structures with carbon fiber plain weave skins and a Nomex core.[58] Although the use of randomly oriented CF/PEKK strands leads to variations in strand orientation within the recycled skins (Figure 11B), it yields a low standard deviation of 3.77 in the average impact energy value of the sandwich composite structures.

Additionally, Figure 11C–F present the micrographs of fractured Charpy impact specimens. As can be seen from the lateral surfaces of the sandwich composite, the upper skin (Figure 11C) and the lower skin (Figure 11D) exhibit a similar failure behavior where inter-strand debonding, strand splitting, and plastic deformation take place. This is interesting because during the impact, the upper skin is subjected to compressive stress while the lower skin is subjected to tensile stress. The reason behind this is the discontinuity and the randomness of the CFs which makes the aforementioned failure modes less energy demanding. Additionally, the inter-strand debonding is accompanied by significant plastic deformation, evident from the formation of cusps and the rough fracture surface at the strand boundaries as shown in Figure 11E. Moreover, Figure 11F shows that core material fails under compression, as apparent from the kinking of the cell walls of the core. This is because inter-strand debonding and strand splitting cause stress relaxation in the skin/core interface, which minimizes in-plane shear stress.

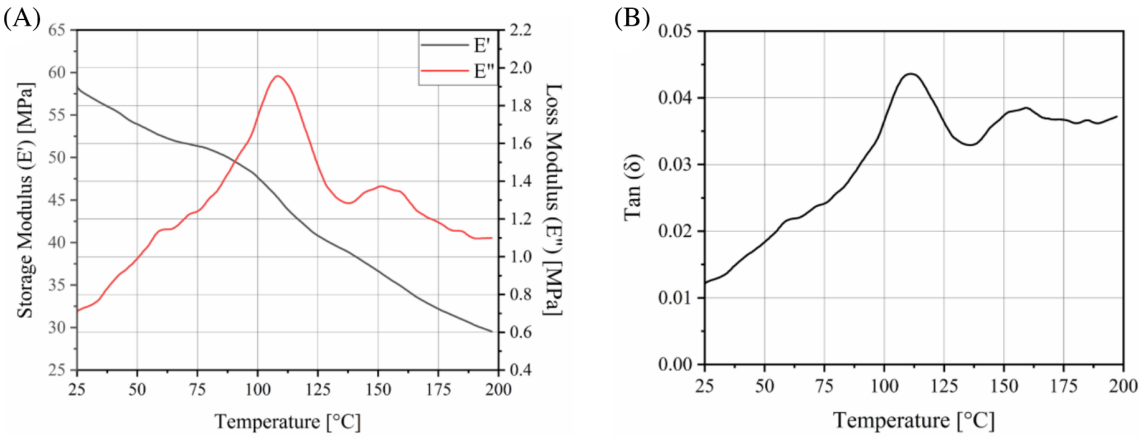

FIGURE 12 The results of dynamic mechanical analysis: (A) Storage and loss moduli and (B) tan (δ) values of the sandwich composite structure.

3.6 | Dynamic mechanical analysis

The dynamic mechanical analysis (DMA) results of the sandwich composite specimen are presented in Figure 12. In Figure 12A, the storage (E') and the loss (E") moduli show that the thermal mechanical response of the specimens is complexly influenced by the combined effects of the thermoplastic skin, the phenolic-based core, and the epoxy-based adhesive film.[59] In the temperature range of 25–60°C, the storage modulus decreases as the mobility of polymer chains increases. As these chains begin to slide past one another, the overall rigidity of the polymeric structure is reduced. Simultaneously, the loss modulus rises, indicating increased internal friction due to chain movement, which results in greater energy dissipation within the material. At around 60°C, the rate of decrease in storage modulus slows before it increases again as the adhesive film and the core material undergo their glass transition. The glass transition temperatures (T_g) of the epoxy resin in the structural adhesive and the phenolic resin in the core material occur in close proximity, as indicated by the overlapping loss modulus peak around 108°C. This thermal behavior suggests a similar transition range for both materials, which is reported in the literature.[59] After the glass transition of the core and the adhesive, the storage modulus continues to decrease, and the loss modulus forms another peak at around 150°C as the CF/PEKK reaches its glass transition temperature. These results are also reflected in the tan (δ) values (Figure 12B) where tan (δ) exhibits a positive trend until the glass transition temperature of the core and the adhesive film. As the energy dissipation decreases after the glass transition of the core and the adhesive film, tan (δ) values decrease before they increase again due to the CF/PEKK skins undergoing their glass transition.

4 | CONCLUSION

The integration of recycled composite skin in sandwich structures provides environmentally friendly, cost-effective, and mechanically efficient characteristics, making it suitable for aerospace applications in secondary load-bearing structures. In this concept, waste CF/PEKK strands are consolidated using a hot press under vacuum bagging to achieve a low void content, which is essential for aerospace structural applications. Integrating the recycled ROS CF/PEKK skins into the sandwich structure proves successful in eliminating the warpage problem due to the enhanced skin/core bonding facilitated by APA. Afterward, a series of test methods, including flatwise, 4-point bending, edgewise compression, Charpy impact, and dynamic mechanical analysis (DMA), are conducted to assess the mechanical performance of the sandwich composite structures. The flatwise tensile test demonstrates the superior bonding performance of the core to the recycled skin, with a strength value of 2.28 MPa. Charpy impact test results in an impact energy value of 49.96 kJ/m^2 which is comparable to sandwich structures with continuous plain weave CF skins. Moreover, a low standard deviation is achieved despite the varying strand orientation of the recycled CF/PEKK. In addition, SEM and stereo microscope images are captured to support the flatwise tensile and Charpy impact test results. The results of the 4-point bending test show that, after the failure of the core material under shear stress, the recycled CF/PEKK skins continue to withstand loads until the fracture point. Upon examination of the edgewise compression specimens, various failure modes, skin failure under compression, and core failure due to buckling, are observed. In the DMA, the lower glass transition temperature (T_g) of the honeycomb core material causes the storage modulus of the sandwich composite structure to decrease rapidly. The overall assessment provided in this study demonstrates that integrating

ROS composites into sandwich structures as skin materials can eliminate geometrical instability due to warpage. Additionally, sandwich structures with ROS composite skins provide a mechanical performance suitable for aerospace secondary load-bearing applications.

ACKNOWLEDGMENTS

This work is supported by the Scientific and Technological Research Council of Turkey (TUBITAK) under the grant of 2244 Research Projects Program (TUBITAK Project no: 118C051) and by Çanakkale Onsekiz Mart University, the scientific research coordination unit, project no: FYL-2020-3375. The authors would like to express their gratitude to TÜBİTAK for their support. Additionally, we wish to thank KORDSA for their generous donation of the slit tape and honeycomb Nomex materials.

DATA AVAILABILITY STATEMENT

Data will be made available upon request.

ORCID

Yağız Özbek https://orcid.org/0000-0002-6194-1467
Sinem Elmas https://orcid.org/0000-0002-9745-9680
Volkan Eskizeybek https://orcid.org/0000-0002-5373-0379
Mehmet Yıldız https://orcid.org/0000-0003-1626-5858

REFERENCES

1. Le VT, Ha NS, Goo NS. Advanced sandwich structures for thermal protection systems in hypersonic vehicles: a review. *Compos Part B: Eng*. 2021;226:109301. doi:10.1016/J.COMPOSITESB.2021.109301
2. Castanie B, Bouvet C, Ginot M. Review of composite sandwich structure in aeronautic applications. *Compos Part C: Open Access*. 2020;1:100004. doi:10.1016/J.JCOMC.2020.100004
3. Seyyed Monfared Zanjani J, Yousefi Louyeh P, Emami Tabrizi I, Al-Nadhari AS, Yildiz M. Thermo-responsive and shape-morphing CF/GF composite skin: full-field experimental measurement, theoretical prediction, and finite element analysis. *Thin-Walled Struct*. 2021;160:106874. doi:10.1016/j.tws.2020.106874
4. Prashanth S, Subbaya KM, Nithin K, Sachhidananda S. Fiber reinforced composites—a review. *J Mater Sci Eng*. 2017;6(3):2-6. doi:10.4172/2169-0022.1000341
5. Kausar A, Ahmad I, Rakha SA, Eisa MH, Diallo A. State-of-the-art of Sandwich composite structures: manufacturing-to-high performance applications. *J Compos Sci*. 2023;7(3):102. doi:10.3390/jcs7030102
6. Gao X, Zhang M, Huang Y, Sang L, Hou W. Experimental and numerical investigation of thermoplastic honeycomb sandwich structures under bending loading. *Thin-Walled Struct*. 2020;155:106961. doi:10.1016/J.TWS.2020.106961
7. Grünewald J, Parlevliet P, Altstädt V. Manufacturing of thermoplastic composite sandwich structures: a review of literature. *J Thermoplast Compos Mater*. 2017;30(4):437-464. doi:10.1177/0892705715604681/ASSET/IMAGES/LARGE/10.1177_0892705715604681-FIG13.JPEG
8. He M, Hu W. A study on composite honeycomb sandwich panel structure. *Mater Des*. 2008;29(3):709-713. doi:10.1016/J.MATDES.2007.03.003
9. Hsu DK. Non-destructive evaluation (NDE) of aerospace composites: ultrasonic techniques. *Non-Destructive Evaluation (NDE) of Polymer Matrix Composites*. Elsevier; 2013:397-422. doi:10.1533/9780857093554.3.397
10. Foo CC, Chai GB, Seah LK. Mechanical properties of Nomex material and Nomex honeycomb structure. *Compos Struct*. 2007;80(4):588-594. doi:10.1016/J.COMPSTRUCT.2006.07.010
11. Niknafs Kermani N, Simacek P, Advani SG. A bond-line porosity model that integrates fillet shape and prepreg facesheet consolidation during equilibrated co-cure of sandwich composite structures. *Compos Part A: Appl Sci Manuf*. 2020;139:106071. doi:10.1016/j.compositesa.2020.106071
12. Chen C, Li Y, Gu Y, Li M, Zhang Z. Improvement in skin-core adhesion of multiwalled carbon nanotubes modified carbon fiber prepreg/Nomex honeycomb sandwich composites. *J Reinf Plast Compos*. 2017;36(8):608-618. doi:10.1177/0731684416687042/ASSET/IMAGES/LARGE/10.1177_0731684416687042-FIG10.JPEG
13. Anders M, Zebrine D, Centea T, Nutt S. In situ observations and pressure measurements for autoclave co-cure of honeycomb core sandwich structures. *J Manuf Sci Eng Trans ASME*. 2017;139(11):1-9. doi:10.1115/1.4037432
14. Grove SM, Popham E, Miles ME. An investigation of the skin/core bond in honeycomb sandwich structures using statistical experimentation techniques. *Compos Part A: Appl Sci Manuf*. 2006;37(5):804-812. doi:10.1016/J.COMPOSITESA.2005.07.005
15. Ozbek Y, Yildirim C, Yakin FE, Topal S, Yildiz M, Sas HS. Enhancing adhesive bonding and mechanical properties of composite sandwich panels through atmospheric plasma activation. *Polym Compos*. 2025;46:5267-5280. doi:10.1002/pc.29290
16. Yildirim C, Ulus H, Beylergil B, Al-Nadhari A, Topal S, Yildiz M. Tailoring adherend surfaces for enhanced bonding in CF/PEKK composites: comparative analysis of atmospheric plasma activation and conventional treatments. *Compos Part A: Appl Sci Manuf*. 2024;180:108101. doi:10.1016/J.COMPOSITESA.2024.108101
17. Sun D, Stylios GK. Effect of low temperature plasma treatment on the scouring and dyeing of natural fabrics. 2004;74(9):751-756. doi:10.1177/004051750407400901
18. Mandegarian S, Hojjati M, Moghaddar H. Thermoplastic composite sandwich panels with recycled PET foam core: a manufacturing process assessment. 2024. doi:10.1177/08927057241291021
19. Kassab R, Sadeghian P. A comparative study on the mechanical properties of sandwich beams made with PET FRP facings and varied recycled PET cores. *Compos Struct*. 2024;344:118340. doi:10.1016/J.COMPSTRUCT.2024.118340
20. Hu J, Zhu S, Wang B, et al. Fabrication and compression properties of continuous carbon fiber reinforced polyether ether ketone thermoplastic composite sandwich structures with lattice cores. *J Sandw Struct Mater*. 2021;23(6):2422-2442. doi:10.1177/1099636220909949
21. Martin RG, Johansson C, Tavares JR, Dubé M. Manufacturing of thermoplastic composite sandwich panels using induction welding under vacuum. *Compos Part A: Appl Sci Manuf*. 2024;182:108211. doi:10.1016/J.COMPOSITESA.2024.108211
22. Shi H, Liu W, Fang H. Damage characteristics analysis of GFRP-balsa sandwich beams under four-point fatigue bending.

Compos Part A: Appl Sci Manuf. 2018;109:564-577. doi:10.1016/J.COMPOSITESA.2018.04.005

23. Bajurko P. Comparison of damage resistance of thermoplastic and thermoset carbon fibre-reinforced composites. *J Thermoplast Compos Mater*. 2021;34(3):303-315. doi:10.1177/0892705719844550
24. Elmas S, Atac B, Senol CO, Topal S, Yildiz M, Sas HS. Annealing impact on mechanical performance and failure analysis assisted with acoustic inspection of carbon fiber reinforced poly-ether-ketone-ketone composites under flexural and compressive loads. *Polym Compos*. 2025;46:3686-3704. doi:10.1002/PC.29199
25. Erland S, Stevens H, Savage L. The re-manufacture and repairability of poly(ether ether ketone) discontinuous carbon fibre composites. *Polym Int*. 2021;70(8):1118-1127. doi:10.1002/pi.6220
26. Henshaw JM. Recycling and disposal of polymer-matrix composites. *Composites*. 2001;21:1006-1012. doi:10.31399/ASM.HB.V21.A0003471
27. Qiao Y, Fring LD, Pallaka MR, Simmons KL. A review of the fabrication methods and mechanical behavior of continuous thermoplastic polymer fiber–thermoplastic polymer matrix composites. *Polym Compos*. 2023;44(2):694-733. doi:10.1002/PC.27139
28. Krauklis AE, Karl CW, Gagani AI, et al. Composite material recycling technology—state-of-the-art and sustainable development for the 2020s. *J Compos Sci 2021*. 2021;5(1):28. doi:10.3390/JCS5010028
29. Fernandes H, Zhang H, Ibarra-Castanedo C, Maldague X. Fiber orientation assessment on randomly-oriented strand composites by means of infrared thermography. *Compos Sci Technol*. 2015;121:25-33. doi:10.1016/J.COMPSCITECH.2015.10.015
30. Wang Y, Savage L. Manufacturing of pre-impregnated discontinuous PAEK/CF composite.Proceedings of the 21st international conference on composite materials. 2017.
31. Yildirim C, Tabrizi IE, Al-Nadhari A, Topal S, Beylergil B, Yildiz M. Characterizing damage evolution of CF/PEKK composites under tensile loading through multi-instrument structural health monitoring techniques. *Compos Part A: Appl Sci Manuf*. 2023;175(August):107817. doi:10.1016/j.compositesa.2023.107817
32. Selezneva M, Lessard L. Characterization of mechanical properties of randomly oriented strand thermoplastic composites. *J Compos Mater*. 2016;50(20):2833-2851. doi:10.1177/0021998315613129
33. Leblanc D, Landry B, Jancik M, Hubert P. Recyclability of randomly-oriented strand thermoplastic composites. Proceedings of the 20th international conference on composite materials. 2015.
34. Eguémann N, Giger L, Masania K, Dransfeld C, Thiebaud F, Perreux D. Processing of characterisation of carbon fibre reinforced peek with discontinuous architecture. Proceedings of the 16th European conference on composite materials. 2014.
35. Collins C, Batista NL, Hubert P. Warpage investigation of carbon/PEEK discontinuous long fibre thin panels. *J Compos Mater*. 2021;55(24):3529-3537. doi:10.1177/00219983211002247
36. Visweswaraiah SB, Lessard L, Hubert P. Tensile behaviour of hybrid fibre architectures of randomly oriented strands combined with laminate groups. *J Compos Mater*. 2019;53(26–27):3725-3740. doi:10.1177/0021998319844590
37. Barzegar A, Karimi S, Sukur EF, Sas HS, Yildiz M. Effect of fiber orientation on temperature history during laser-assisted thermoplastic fiber placement. *J Reinf Plast Compos*. 2023;42(17–18):953-968. doi:10.1177/07316844221143448
38. Toray Cetex® TC1320 PEKK. *Product Data Sheet. Product Type PEKK (PolyEtherKetoneKetone) Thermoplastic Resin System Shelf Life Typical Neat Resin Properties*. Torray Advanced Composites; 2022.
39. Aerospace Grade Nomex® Honeycomb. AXIOM materials. https://axiommaterials.com/products/aerospace-grade-nomex-honeycomb/
40. Scotch-Weld 3M. Technical datasheet AF 163-2 structural adhesive film. 2009.
41. Özbek Y, Al-Nadhari A, Eskizeybek V, Yıldız M, Şaş HS. Influence of Strand size and morphology on the mechanical performance of recycled CF/PEKK composites: harnessing waste for aerospace secondary load-bearing applications. *Compos Part B: Eng*. 2025;296:112232. doi:10.1016/j.compositesb.2025.112232
42. Marasco AI, Cartié DDR, Partridge IK, Rezai A. Mechanical properties balance in novel Z-pinned sandwich panels: out-of-plane properties. *Compos Part A: Appl Sci Manuf*. 2006;37(2):295-302. doi:10.1016/j.compositesa.2005.03.029
43. Ulus H, Kaybal HB, Cacık F, Eskizeybek V, Avcı A. Fracture and dynamic mechanical analysis of seawater aged aluminum-BFRP hybrid adhesive joints. *Eng Fract Mech*. 2022;268(January):108507. doi:10.1016/j.engfracmech.2022.108507
44. Ahmad S, Zhang J, Feng P, Yu D, Wu Z, Ke M. Processing technologies for Nomex honeycomb composites (NHCs): a critical review. *Compos Struct*. 2020;250:112545. doi:10.1016/j.compstruct.2020.112545
45. Singh MK, Singh A. *Characterization of Polymers and Fibers*. Woodhead Publishing; 2021.
46. Khan S, Loken HY. Bonding of sandwich structures—the facesheet/honeycomb interface: a phenomenological study. Proceedings of SAMPE. 2007.
47. Roy R, Nguyen KH, Park YB, Kweon JH, Choi JH. Testing and modeling of Nomex™ honeycomb sandwich panels with bolt insert. *Compos Part B: Eng*. 2014;56:762-769. doi:10.1016/j.compositesb.2013.09.006
48. Liu L, Wang H, Guan Z. Experimental and numerical study on the mechanical response of Nomex honeycomb core under transverse loading. *Compos Struct*. 2015;121:304-314. doi:10.1016/j.compstruct.2014.11.034
49. Yildirim C, Ulus H, Beylergil B, Al-Nadhari A, Topal S, Yildiz M. Effect of atmospheric plasma treatment on mode-I and mode-II fracture toughness properties of adhesively bonded carbon fiber/PEKK composite joints. *Eng Fract Mech*. 2023;289-(March):109463. doi:10.1016/j.engfracmech.2023.109463
50. Manalo AC, Aravinthan T, Karunasena W, Islam MM. Flexural behaviour of structural fibre composite sandwich beams in flatwise and edgewise positions. *Compos Struct*. 2010;92(4):984-995. doi:10.1016/j.compstruct.2009.09.046
51. Tagarielli VL, Fleck NA, Deshpande VS. Collapse of clamped and simply supported composite sandwich beams in three-point bending. *Compos Part B: Eng*. 2004;35(6–8):523-534. doi:10.1016/j.compositesb.2003.07.001
52. Russo A, Zuccarello B. Experimental and numerical evaluation of the mechanical behaviour of GFRP sandwich panels. *Compos Struct*. 2007;81(4):575-586. doi:10.1016/j.compstruct.2006.10.007

53. Bekuit JJRB, Oguamanam DCD, Damisa O. A quasi-2D finite element formulation for the analysis of sandwich beams. *Finite Elem Anal Des*. 2007;43(14):1099-1107. doi:10.1016/j.finel.2007.08.005
54. Naresh K, Alia RA, Cantwell WJ, Umer R, Khan KA. Influence of face sheet thickness on flexural strength characteristics of carbon/epoxy/Nomex honeycomb sandwich panels. *J Sandw Struct Mater*. 2023;25(5):537-554. doi:10.1177/10996362231159925
55. Zhu S, Wang Y, Zhou L, et al. Experimental investigation on mechanical behaviors of composite sandwich panels with a hybrid facesheet. *Polym Compos*. 2023;44(6):3196-3208. doi:10.1002/pc.27311
56. Florence A, Jaswin MA, Arul Prakash MDA, Jayaram RS. Effect of energy-absorbing materials on the mechanical behaviour of hybrid FRP honeycomb core sandwich composites. *Mater Res Innov*. 2020;24(4):244-255. doi:10.1080/14328917.2019.1640497
57. Evci C, Gülgeç M. An experimental investigation on the impact response of composite materials. *Int J Impact Eng*. 2012;43:40-51. doi:10.1016/j.ijimpeng.2011.11.009
58. Zaharia SM, Pop MA, Semenescu A, Florea B, Chivu OR. Mechanical properties and fatigue performances on sandwich structures with CFRP skin and nomex honeycomb core. *Mater Plast*. 2017;54(1):67-72. doi:10.37358/mp.17.1.4788
59. Redmann A, Montoya-ospina MC, Karl R, Rudolph N, Osswald TA. High-force dynamic mechanical analysis of composite sandwich panels for aerospace structures. *Compos Part C: Open Access*. 2021;5:100136. doi:10.1016/j.jcomc.2021.100136

SUPPORTING INFORMATION

Additional supporting information can be found online in the Supporting Information section at the end of this article.

How to cite this article: Özbek Y, Al-Nadhari A, Elmas S, Eskizeybek V, Yıldız M, Sas HS. Feasibility and performance evaluation of randomly oriented strand recycled composite skins in sandwich structures: A green cost-effective solution for aerospace secondary load-bearing applications. *Polym Compos*. 2025;46(12):11341-11357. doi:10.1002/pc.29689